TOXICOLOGY AND APPLIED PHARMACOLOGY 132, 103–114 (1995)

Development of a Physiologically Based Pharmacokinetic Model Describing 2-Methoxyacetic Acid Disposition in the Pregnant Mouse[1]

KETTI K. TERRY,[2] BARBARA A. ELSWICK, FRANK WELSCH,[3] AND RORY B. CONOLLY

Chemical Industry Institute of Toxicology, P.O. Box 12137, Research Triangle Park, North Carolina 27709

Received June 14, 1994; accepted November 29, 1994

Development of a Physiologically Based Pharmacokinetic Model Describing 2-Methoxyacetic Acid Disposition in the Pregnant Mouse. TERRY, K. K., ELSWICK, B. A., WELSCH, F., AND CONOLLY, R. B. (1995). *Toxicol. Appl. Pharmacol.* 132, 103–114.

Using the potent developmental toxicant 2-methoxyethanol (2-ME) as a prototypical compound, a physiologically based pharmacokinetic (PBPK) model was developed to describe the disposition of its primary metabolite and proximate toxicant 2-methoxyacetic acid (2-MAA) in the pregnant CD-1 mouse. Data were collected during early, mid, and late organogenesis, specifically Gestation Days (GD) 8, 11, and 13 (GD 0 = plug-positive date). Pharmacokinetics and tissue partition coefficients for 2-MAA were determined in maternal plasma and conceptus on GD 8 and in maternal plasma, embryo, and extraembryonic/amniotic fluid (EAF) on GD 11 and 13. For simulation of GD 8 data, the conceptus was described as a single compartment, combining the yolk sac placenta, embryo, EAF, and decidua. For GD 11 and 13, the placenta, embryo, and EAF were explicitly described. Several hypotheses were tested for their ability to predict 2-MAA dosimetry. These hypotheses were encoded as alternative models having (a) blood flow-limited delivery of 2-MAA to model compartments, (b) pH trapping of ionized 2-MAA within compartments, (c) active transport of 2-MAA into compartments, and (d) reversible binding of 2-MAA within compartments. While the flow-limited description adequately predicted GD 8 dosimetry, the best simulations of the pharmacokinetic data collected on GD 11 and 13 were obtained with the active transport models. Since the mechanism by which 2-MAA accumulates into the embryo and EAF has not yet been elucidated, these mathematical descriptions are empirical. Further development of this PBPK model for 2-MAA in pregnant mice, in particular its scale-up to humans, will facilitate more realistic human risk assessments for the developmental toxicity of 2-ME and related compounds. © 1995 Academic Press, Inc.

Development of mechanism-based, quantitative dosimetry models that accurately predict chemical disposition in laboratory animals is an important component of the effort to improve exposure–response assessments. Classical dosimetry models are typically based on the curve fitting of multiexponential model equations to plasma-concentration time data (Gabrielsson and Paalzow, 1983; Gabrielsson and Larsson, 1987; for reviews see Himmelstein and Lutz, 1979; Conolly and Andersen, 1991). Although classical models are useful for some pharmacokinetic studies, they do not explicitly describe the physiological system that determines pharmacokinetic behavior. Such models do not provide information on, for example, tissue-to-tissue concentration differences, the effect of diffusion limitation, or changes in protein binding (Gabrielsson and Larsson, 1987).

Limitations of the classical models led to the need for more realistic descriptions (Gabrielsson and Larsson, 1987). In physiologically based pharmacokinetic (PBPK) models, the compartments represent the physical structure of the organism. Chemical dosimetry is defined realistically in terms of tissues, blood flows, excretion rates, reaction pathways, tissue solubilities, and binding properties (Conolly and Andersen, 1991). To describe pregnancy, O'Flaherty *et al.* (1992) developed a PBPK model of rodent gestation that incorporates growth and aging of the dam and conceptus. In that model, pregnancy-induced changes in maternal tissue volumes and blood flows, as well as growth of the embryo/fetus, are depicted from conception to parturition. Development of a PBPK model that describes chemical disposition in the gestating rodent is a necessary precursor for similar efforts with other species, including humans.

A few mathematical models have been developed to simulate the dosimetry of drugs and other chemicals in pregnant rodents. Experimental compounds include tetracycline (Olanoff and Anderson, 1980), morphine (Gabrielsson and Paalzow, 1983), theophylline, methadone, and

[1] Presented in part at the annual meetings of the Teratology Society (Boca Raton, FL, 1992 and Tucson, AZ, 1993), the First Annual U.S. EPA Health Effects Research Laboratory Symposium ("Biological Mechanisms and Quantitative Risk Assessment," U.S. EPA, Research Triangle Park, NC, 1993), and the meeting of the Society of Toxicology (Dallas, TX, 1994).

[2] Present address: National Center for Toxicological Research, Division of Reproductive & Developmental Toxicology, USFDA, Jefferson, AR 72079.

[3] To whom correspondence and reprint requests should be addressed. Fax: (919) 558-1300.

0041-008X/95 $6.00

pethidine (Gabrielsson *et al.*, 1984, 1985, 1986), salicylic acid (Gabrielsson and Larsson, 1987), trichloroethylene (Fisher *et al.*, 1989), and dimethyloxazolidine-2,4-dione (DMO; O'Flaherty *et al.*, 1992). All but the DMO description predict chemical dosimetry during late stages of pregnancy when fetogenesis and organ maturation are ongoing. Only the PBPK model by O'Flaherty and co-workers (1992) incorporates the physiological changes occurring in the dam and conceptus during the entire gestation period. Since organogenesis spans the developmental phase most susceptible to teratogenic insult, accurate prediction of chemical disposition at this time is imperative for the development of useful risk assessment models applicable to pregnant women who are exposed to potentially toxic chemicals.

Recently, Clarke and colleagues (1993) developed and validated a PBPK model for 2-methoxyacetic acid (2-MAA), the primary metabolite and proximate toxicant of 2-methoxyethanol (2-ME; Brown *et al.*, 1984; Yonemoto *et al.*, 1984; Ritter *et al.*, 1985; Sleet *et al.*, 1988). In that model quantitative descriptions of physiologic changes occurring throughout gestation as determined by O'Flaherty *et al.* (1992) served as the template onto which a description of 2-ME/2-MAA pharmacokinetics in the pregnant CD-1 mouse was superimposed (Clarke *et al.*, 1993). The resulting PBPK model successfully simulated the pharmacokinetic behavior of 2-ME and 2-MAA in maternal plasma, embryo, and extraembryonic/amniotic fluid in Gestation Day (GD) 11 mice (Clarke *et al.*, 1993). Limited pharmacokinetic data for other gestation times, however, precluded adequate validation of the model's ability to simulate 2-MAA disposition at different developmental stages.

The present study focused on simulating the disposition of 2-MAA during early, middle, and relatively late mouse organogenesis (GD 8, 11, and 13). The objective of this study was to expand the pharmacokinetic data base and to test several hypotheses concerning the biochemical mechanism(s) of 2-MAA disposition.

METHODS

Details of the procedures for the determination of 2-MAA pharmacokinetics, tissue partitioning, metabolic parameters, and disposition of 2-ME were reported by Clarke *et al.* (1993). In the present study, most of the anatomical and metabolic parameters remained as reported by those authors (Table 1).

Animals

Male and female Crl:CD-1 ICR BR (CD-1) mice, 8 to 10 weeks old, were purchased from the Charles River Breeding Laboratories (Raleigh, NC). Mice were housed and bred in a mass air displacement room (Bioclean, Hazleton Systems, Vienna, VA), maintained at 22 ± 1.5°C, 50 ± 10% relative humidity, with a 12-hr light cycle beginning at 0900 hours. Female mice were caged in groups of five, while males were kept individually. NIH 07 open formula pelleted food (Zeigler Brothers, Gardner, PA) and filtered tap water (Barnsted Nanopure System, Boston, MA) were provided *ad libitum*. During the final 2 hr of the dark cycle nulliparous females (26–36 g) were paired 1:1 in the home cage of the male. Mating was confirmed by the presence of a vaginal plug, and the following 24-hr period was designated GD 0.

TABLE 1
Anatomical and Kinetic Parameters for CD-1 Mice Consistent with Those in the Model by Clarke *et al.* (1993)

Adult weight (g)	30.00
Pup weight at birth (g)	1.34
Gestation time (days)	19.00
Average litter size	12.8
Early growth constant	0.165

Tissue partition coefficients	2-ME	2-MAA
Blood/reference[a]	34,913	0.99
Liver/blood[b]	1.02	nr
Fat/blood	0.05	nr
Poorly perfused tissue/blood	0.93	nr

2-ME pharmacokinetic constants

V'_{maxMAA} (mmol·day^{-1})	$24 \times 2.40 \times$ body wt$^{0.74}$
K_{mMAA} (mmol·liter^{-1})	0.15
V'_{maxFG} (mmol·day^{-1})	$24 \times 0.16 \times$ body wt$^{0.74}$
K_{mFG} (mmol·liter^{-1})	0.0083

2-MAA pharmacokinetic constants

V_d (liter)	0.510 × body wt
ke (day^{-1})	24×0.0342/body wt$^{0.26}$
kf (day^{-1})	24×0.0195/body wt$^{0.26}$

Note. nr, not required for current model.
[a] Air for 2-ME PCs, saline for 2-MAA PCs.
[b] Also represents PC for other richly perfused tissues/blood (Clarke *et al.*, 1993).

Chemicals

2-ME and 2-MAA (each 99.9% pure) were purchased from Aldrich Chemical Co. (Milwaukee, WI) and Eastman Kodak Co. (Rochester, NY), respectively. [1,2-^{14}C]2-Methoxyethanol ([^{14}C]2-ME; specific activity 7.4 mCi/mmol) and 2-methoxy-[1-^{14}C]acetic acid ([1-^{14}C]2-MAA; specific activity 5.0 mCi/mmol) were custom synthesized and had a radiochemical purity of 98% (Wizard Laboratories, Davis, CA).

Tissue Samples

Data for 2-MAA partition coefficients and tissue dosimetry were obtained on GD 8, 11, and 13. Maternal plasma was collected from all mice. The GD 8 conceptus sample consisted of the combined embryo, extraembryonic/amniotic fluid (EAF), yolk sac, and decidual swelling as in other studies (Nau, 1985; Wegner and Nau, 1992; Terry *et al.*, 1994). On GD 11 and 13 embryos were collected separately and each litter was pooled for analysis. EAF samples were obtained in the same manner.

Pharmacokinetics

2-MAA dosimetry data used for model development were obtained in GD 8 maternal plasma and conceptuses following an iv administration of 2-ME (Terry *et al.*, 1994). Data for GD 11 maternal plasma, embryo, and EAF were determined following a bolus oral (po) 2-ME dose (Clarke *et*

al., 1993). In the present study, GD 13 pharmacokinetics of 2-MAA were determined in plasma, embryo, and EAF following an iv bolus injection of 2-ME into the lateral tail vein. In all experiments for each GD, 250 mg 2-ME/kg was administered combined with about 4 mCi [^{14}C]2-ME per mouse between 0800 and 1000 hours. A constant dosing volume of 2.6 and 5.2 ml/g was used for the iv bolus and po doses, respectively.

On GD 13, 2-MAA was determined at various time points following 2-ME administration (0.083, 0.25, 0.5 0.75, 1.0, 1.5, 3, 6, 12, and 24 hr). At each time point, samples were taken from three to five animals. In isotope dilution experiments with [^{14}C]2-ME, separation of 2-ME and 2-MAA was achieved by injecting extracts onto a 15-cm PRP×300 column (Hamilton, Reno, NV) connected to a Spectroflow 400 HPLC (ABI Analytical Division, Columbia, MD). Radioactivity was quantitated with a Flow-one Beta radioactivity detector and software (Radiomatic Institute & Chemical Co., Tampa, FL).

2-MAA Partition Coefficients (PCs)

Since 2-MAA is nonvolatile, a centrifugal ultrafiltration technique employing [1-^{14}C]2-MAA (Jepson *et al.*, 1994) was used. The measured PCs applied in the present study included whole blood/saline and conceptus/saline on GD 8, as well as blood/saline, placenta/blood, embryo/blood, and EAF/blood on GD 11 were measured previously (Clarke *et al.*, 1993). The tissue/blood PCs were calculated by dividing the tissue/saline values by the 2-MAA blood/saline value.

PBPK Model

The equations describing changes in maternal organ (tissue) volumes and blood flows, growth of the yolk sac, and chorioallantoic placentas, as well as development of the embryo, that occur during rodent gestation were essentially those published by O'Flaherty *et al.* (1992). In that model, species conversions from rat to mouse are carried out in the conventional manner by scaling rates and clearances with body weight to the power of 0.74. However, the body weights of the conceptuses (embryo/fetuses) and the blood flows associated with those tissues were not conventionally scaled. The species-specific differences in gestational length and birth weight of the pups were applied to determine the rate of growth of the embryo/fetus (O'Flaherty *et al.*, 1992). CD-1 mouse strain-specific information was added regarding weight of a young adult, female's age on Day 1 of pregnancy, pup weight at birth, and mean litter size (Clarke *et al.*, 1993). Values of model parameters were obtained from several sources that are listed in detail in Appendix II.

Disposition of 2-ME

The PBPK model for 2-ME included maternal compartments for fat, poorly perfused tissue (including muscle, skin, and bone), richly perfused tissue (including kidney, intestines, mammary glands, uterus, and conceptus), and liver (Fig. 1). A flow-limited discription of 2-ME transfer between maternal plasma and the body tissues was used, and metabolic conversion of 2-ME to 2-MAA and ethylene glycol (EG) was described in the liver (Fig. 1, Table 1; Clarke *et al.*, 1993).

Disposition of 2-MAA

Once 2-MAA leaves the liver, it circulates in the dam (represented for 2-MAA dosimetry as a single compartment) and into the embryonic compartments. For all model versions, the concentration of 2-MAA in maternal plasma (corresponding to the concentration in the volume of distribution) was predicted from (a) the rate of 2-MAA production from 2-ME, (b) a first-order elimination rate for 2-MAA, (c) changes in the volume of distribution related to pregnancy, and (d) the net flow of 2-MAA to and from the conceptus.

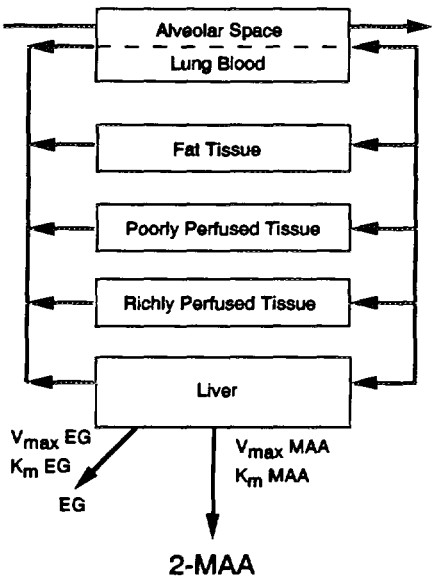

FIG. 1. Physiologically based pharmacokinetic model for 2-ME in the dam. 2-ME is metabolized in the liver to ethylene glycol (EG) and 2-methoxyacetic acid (2-MAA).

Model-Derived Weights

Model-derived weights of conceptuses and their component tissues were validated between GD 7 and 18 (Clarke *et al.*, 1993). At early periods, specifically between GD 7 and 9, the physiological pregnancy model incorporated the decidua in the combined weight of the yolk sac and embryo proper (Clarke *et al.*, 1993). Hence, all of the components in the GD 8 conceptus sample were represented in the model.

Model Development

As described above, on GD 8 it was only possible to obtain tissue samples consisting of combined embryo, EAF, yolk sac, and decidual swelling. By GD 11, growth of the conceptus allowed collection of separate samples of EAF and embryo. Accordingly, the model used to simulate 2-MAA pharmacokinetic data for GD 8 consisted of a single conceptus compartment, while the models for GD 11 and 13 had separate embryo, EAF, and placenta compartments. Details of the equations used for the pharmacokinetic models described in the following section are given in Appendix I.

Flow-limited 2-MAA pharmacokinetics. Blood flow-limited delivery of 2-MAA was assumed for the single-compartment model of 2-MAA pharmacokinetics in the GD 8 conceptus (Fig. 2A). Flow-limited delivery was also evaluated for its ability to simulate 2-MAA pharmacokinetic data on GD 11 and 13 (Fig. 2B).

In addition to the flow-limited descriptions, the model by Clarke and coworkers (1993) was reevaluated using the enlarged data base, and several more complex models were examined for their ability to simulate the GD 11 and 13 data.

pH trapping. As a weak organic acid, 2-MAA (pK_a = 3.6) is largely ionized at physiological pH. An equilibrium between the unionized (protonated) and the ionized forms of 2-MAA, based on the Henderson–Hasselbalch equation, was described for maternal blood, embryo, EAF, and placental compartments (Fig. 2C). The unionized form was allowed to move between compartments using flow-limited delivery. The ionized form of 2-MAA was not allowed to move between compartments. The pH values used for the various tissue compartments for both GD 11 and 13 were the same as those used by O'Flaherty *et al.* (1992) for GD 11.

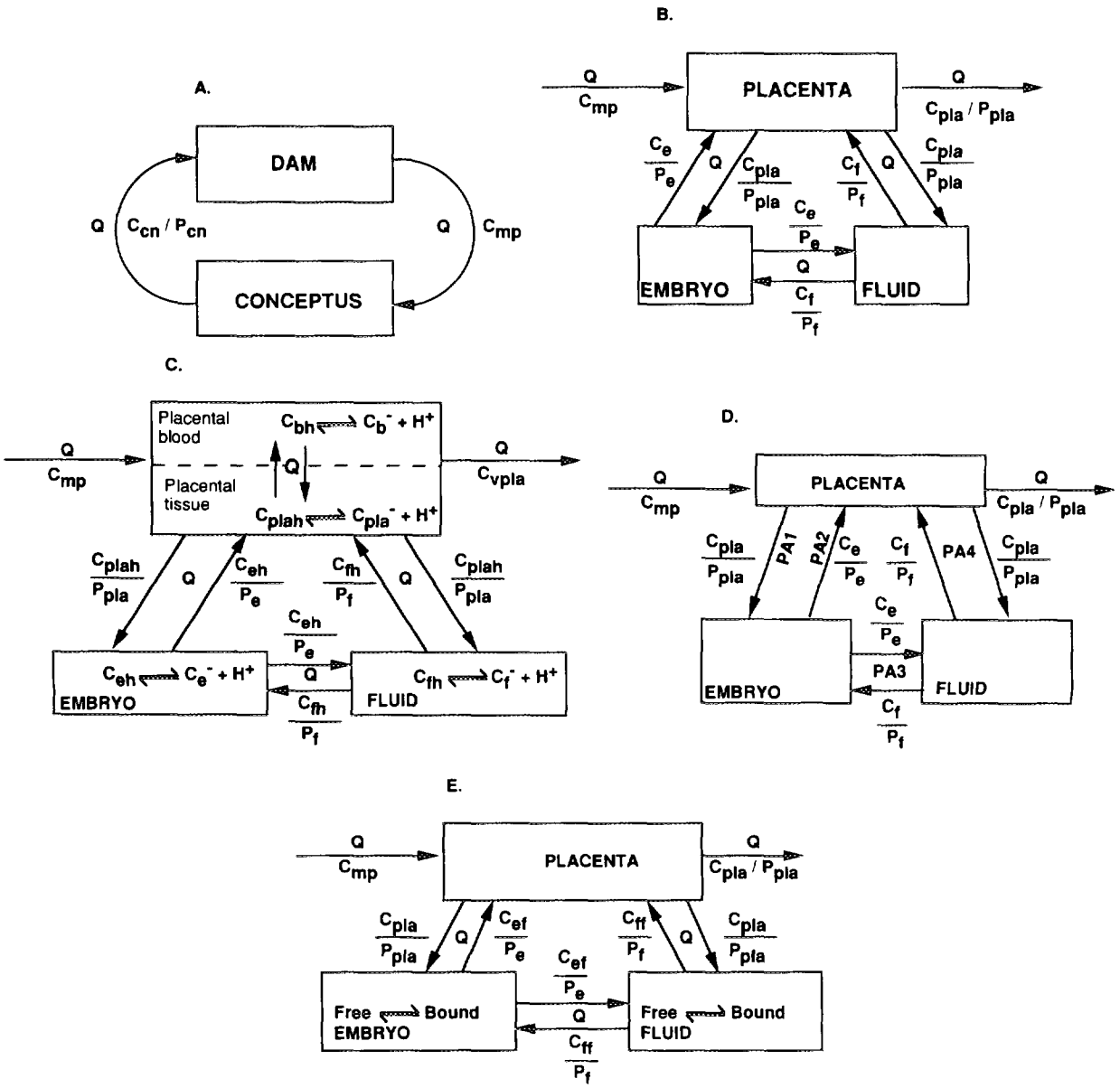

FIG. 2. Model variants for the mouse gestation PBPK model. (A) Flow-limited GD 8 compartmental model for 2-MAA. The dam is represented by a nonphysiological compartment characterized by a volume of distribution for 2-MAA. The blood flow rate, Q, is the placental blood flow rate determined by the physiological model for pregnancy (O'Flaherty *et al.*, 1992). The conceptus compartment, representing the lumped decidua, placenta, embryo, and extraembryonic fluid, has a volume defined by the physiological pregnancy model. (B) Flow-limited GD 11 and 13 model for 2-MAA. Volumes of placenta, embryo, and fluid are determined by the physiological pregnancy model. Flows between compartments (Q) are the same as blood flow to placenta (Q). (C) pH trapping model for 2-MAA on GD 11 and 13. The pH-dependent ionization of 2-MAA is described in placental blood, placenta, embryo, and extraembryonic fluid according to the Henderson–Hasselbalch equation. Only unionized 2-MAA can pass between compartments. Other details as for Fig. 2B. (D) Active transport model for 2-MAA on GD 11 and 13. Model structure as for Fig. 2B, except that flow rates between compartments (PA1–PA4) differ from placental blood flow (Q). Parameters PA1–PA4 were optimized to obtain simulations that fit 2-MAA pharmacokinetic data. (E) Reversible binding model for 2-MAA on GD 11 and 13. Model structure as for Fig. 2B, except that reversible binding of 2-MAA is described in embryo and fluid.

Active transport. Active transport (pumping) was assumed to control movement of 2-MAA between placenta, embryo, and EAF (Fig. 2D).

Reversible binding. Reversible binding of 2-MAA inside the embryo and EAF compartments was described (Fig. 2E). Binding in each compartment was characterized by a binding maximum and dissociation constant. 2-MAA movement between compartments was assumed to be flow-limited, with only the unbound species free to move.

Simulation and optimization. Computer simulations were performed using the SIMUSOLV modeling and simulation program (Mitchell and Gauthier, Concord, MA). Parameter values were initially optimized using

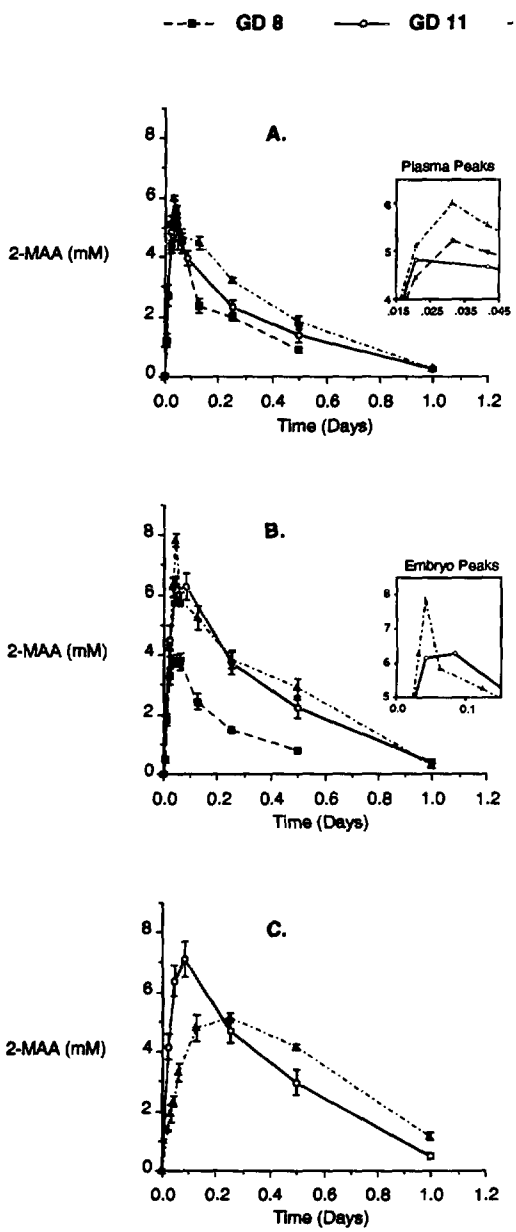

FIG. 3. Tissue dosimetry of 2-MAA in plasma (A), embryo (B), and extraembryonic fluid (EAF; C). A 250-mg 2-ME/kg dose was injected iv on GD 8 or 13 or given by gavage on GD 11. The GD 8 data are from Terry *et al.* (1994), while the GD 11 data are from Clarke *et al.* (1993).

the log likelihood function of SIMUSOLV and then visually optimized to better fit the data.

RESULTS

Pharmacokinetics

Since 2-ME is no longer detectable in maternal plasma by 2 hr after oral exposure, and 2-MAA is the suspected toxicant, only 2-MAA pharmacokinetics are reported here. Little variation existed in maternal plasma 2-MAA kinetics at all three developmental periods (Fig. 3A). Although the elimination phase varied slightly, 2-MAA uptake and peak concentrations (C_{max}) were similar among the gestation times. At each stage the C_{max} values were 5–6 mM and were reached within an hour (Table 2).

When comparing 2-MAA dosimetry in the plasma, embryo, and EAF compartments, complex pharmacokinetic behaviors became apparent. In the GD 8 conceptus, the peak 2-MAA level was significantly lower than that in the GD 8 plasma ($p < 0.05$; Student's t test) (Table 2, Fig. 3). On GD 11, the EAF accumulated 2-MAA to the greatest extent (Table 2, Fig. 3). Peak levels in both GD 11 embryo and EAF were higher than those in the plasma (Table 2, Fig. 3). This contrasts with GD 13 results when 2-MAA achieved the maximum concentration in the embryo, which was significantly higher than the levels found in either maternal plasma or EAF (one-factor ANOVA; $p < 0.05$).

2-MAA Partition Coefficients

The 2-MAA maternal blood/saline partition coefficients obtained on either GD 8 or 13 were similar to the reported GD 11 values (Clarke *et al.*, 1993; Table 3).

Blood Flow to Placenta

Maternal blood flow to the conceptus is modeled as the sum of flows to both yolk sac and chorioallantoic placentas (CAP; O'Flaherty *et al.*, 1992). Blood flow to the placenta, i.e., Q (liter/day), decreases from 0.26 on GD 8 to 0.15 on GD 11, reflecting the marked decrease in flow to the atrophying decidua parietalis more than the augmentation of blood flow delivered to the developing CAP (Buelke-Sam *et al.*, 1982; see Appendix II). Once the CAP is established, blood flow increases more rapidly with gestation age than with the weight of the placenta (Buelke-Sam *et al.*, 1982; O'Flaherty *et al.*, 1992). Hence, O'Flaherty and co-workers (1992) modeled blood flow to the CAP as a power of gestation age, which is why placental blood flow (Q) is larger at

TABLE 2

2-MAA Peak Concentrations in Plasma (mmol/liter), Embryo (mmol/kg), and Extraembryonic/Amniotic Fluid (EAF; mmol/liter) ± SEM Following Administration of 250 mg 2-ME/kg by the Route Indicated

Day	Route	Plasma	Embryo	EAF
8	IV	5.22 ± 0.25	3.81 ± 0.18[a,*]	na
11[b]	PO	4.83 ± 0.57	6.29 ± 0.45	7.12 ± 0.61*
13	IV	6.00 ± 0.09	7.83 ± 0.23*	5.13 ± 0.15*

Note. na, not applicable.

[a] On GD 8 the entire conceptus consisting of embryo, EAF, placenta, and decidua was examined.

[b] Data reported previously (Clarke *et al.*, 1993).

* Significantly different from respective plasma level ($p < 0.05$).

TABLE 3
2-MAA Partition Coefficients[a] Determined on Gestation Days 8, 11, and 13

Day	Blood/saline	Placenta/blood	Embryo/blood	EAF[b]/blood
8	1.06	*na*	1.07[c]	*na*
11[d]	0.99	1.05	0.94	1.33
13	1.12	1.33	1.26	1.11

Note. na, not applicable.

[a] The coefficient of variation around the mean of all values ranged from 5 to 16%.

[b] EAF, extraembryonic/amniotic fluid.

[c] For the Gestation Day 8 conceptus, a conceptus/blood partition coefficient was determined where the conceptus included the embryo, EAF, yolk sac placenta, and decidual swelling.

[d] Data reported previously (Clarke *et al.*, 1993).

GD 13 (0.29 liter/day) than at GD 11 (0.15 liter/day; see Appendix II).

Model Discrimination

Flow-limited, single compartment model for the GD 8 conceptus. This model, describing flow-limited delivery of 2-MAA on GD 8 (Fig. 2A), produced adequate simulations of both maternal plasma and conceptus data, although it overpredicted the conceptus C_{max} by about 30% (Figs. 4A and B).

Evaluation of the model described by Clarke et al. (1993) for GD 11 and 13. Although this model produced satisfactory simulations of GD 11 data, it failed to accurately simulate GD 13 kinetics of 2-MAA (simulations not shown). The published model generated good fits to GD 13 plasma and EAF data but underestimated the peak embryo concentrations by 50%. Efforts to simulate the higher 2-MAA levels in GD 13 embryos led to overprediction of 2-MAA concentration in the EAF. For example, simulations reaching 6 mM in the embryo (20% less than the actual C_{max} of 7.83 mM) resulted in a simulated EAF C_{max} of 9.0 mM (180% the actual peak of 5.13 mM).

Flow-limited, multicompartment model for GD 11 and 13. At both gestation days, this model (Fig. 2B) accurately simulated maternal plasma, however, underpredicting embryo and EAF data by 40 and 20%, respectively (simulations not shown). Wanting to improve the fit in the embryo motivated the development of more complex models described below. These versions accounted for mechanisms that allowed 2-MAA to accumulate in the embryo and EAF to levels not predicted solely on the basis of blood flow and partition coefficients, as is the case with the flow-limited models.

pH trapping, multicompartment model for GD 11 and 13. This model (Fig. 2C) failed outright, predicting negligible chemical accumulation in the embryo and EAF at physiological pH (simulations not shown). Accurate simulations (not shown) were only generated in these compartments when nonphysiological pH values of 3 or less were used.

Active transport, multicompartment model for GD 11 and 13. This model (Fig. 2D), describing active transport of 2-MAA, successfully simulated 2-MAA dosimetry on GD 11 and 13 (Fig. 5). Accurate predictions of GD 11 data after 2-ME gavage administration were obtained for all three compartments (Figs. 5A–5C). For GD 13, the model slightly underpredicted the plasma and embryo 2-MAA C_{max} values (by 25 and 16%, respectively), which were determined following iv injections of 2-ME (Figs. 5D and 5E). Although the model-predicted elimination from the EAF compartment on GD 13 was faster than actually measured, simulated values were within acceptable limits of deviation from the biological data, and the C_{max} was accurately obtained (Fig. 5F). Flow parameters for 2-MAA (PA values expressed in liter/day) were optimized and were the same for both GD 11 and 13: PA1 = 1.15, PA2 = 0.63, PA3 = 0.70, and PA4 = 0.30 (see Appendix II).

Reversible binding, multicompartment model for GD 11 and 13. Modeling reversible 2-MAA binding (Fig. 2E) in the embryo and EAF provided reasonable simulations of GD 11 and 13 data (Fig. 6). This model successfully simulated GD 11 data in all three compartments (Figs. 6A–6C). On GD 13, plasma and embryo C_{max} were slightly underestimated by ~25% (Figs. 6D and 6E). The simulated rate of elimination from the EAF compartment was faster than experimentally determined, but the model accurately predicted the C_{max} data determined *in vivo* (Fig. 6F). The simulated binding capacity on both GD 11 and 13 was 0.0008–0.008 mmol, while the simulated dissociation constants were 0.0008 mmol/liter on GD 11 and 0.003 mmol/liter on GD 13. The model describing reversible binding generated predictions similar to those of the active transport model (compare Fig. 5 with Fig. 6).

DISCUSSION

Organogenesis, the time of major organ differentiation and development in embryos, is the period most susceptible

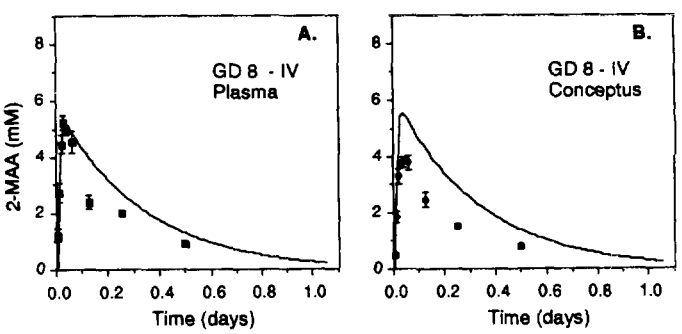

FIG. 4. Flow-limited, GD 8 model simulations (solid line) of 2-MAA pharmacokinetic data represented by the symbols (±SEM) for plasma (A) and conceptus (B) following an iv bolus injection of 250 mg 2-ME/kg.

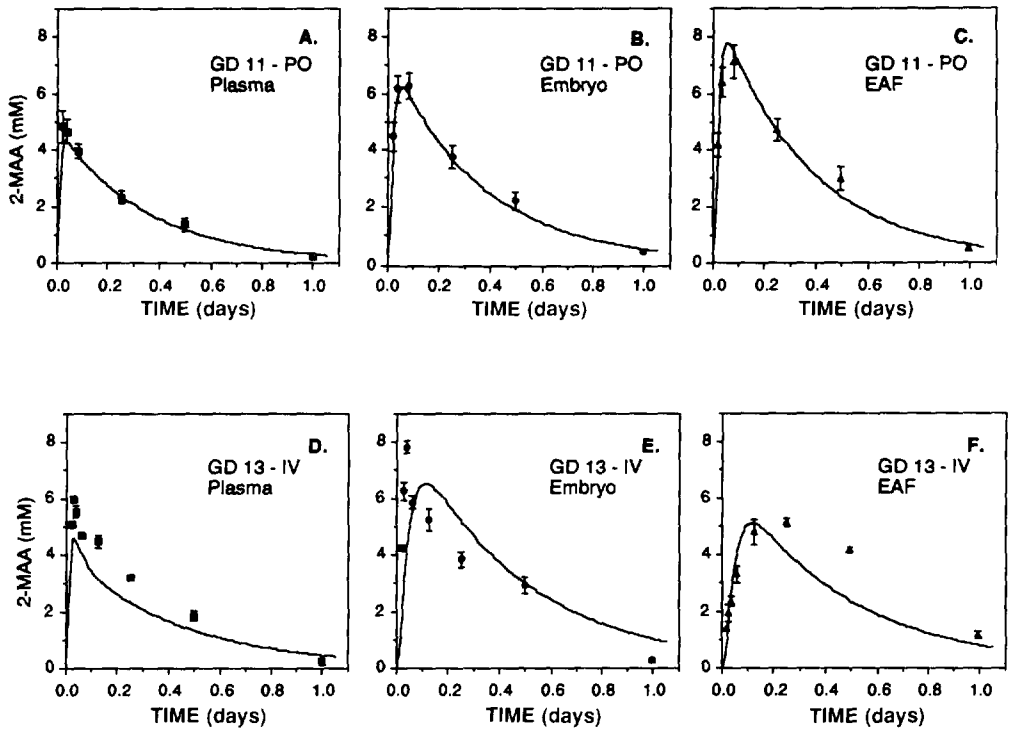

FIG. 5. Active transport model simulations following oral (po) administration of 250 mg 2-ME/kg on GD 11 (A–C) or intravenous (iv) injection on GD 13 (D–F). The solid lines are the simulations of 2-MAA pharmacokinetic data, and the symbols represent the biological data points (±SEM) in plasma (A and F), embryo (B and E), and extraembryonic fluid (EAF; C and E).

to perturbations that may cause maldevelopment. The present study attempted to model quantitatively the disposition of a known developmental toxicant at three different stages of mouse embryogenesis: GD 8, 11, and 13. The chemical teratogen chosen as a prototype was 2-MAA, the primary metabolite and proximate toxicant of 2-ME (Brown *et al.*, 1984; Yonemoto *et al.*, 1984; Ritter *et al.*, 1985; Sleet *et al.*, 1988). Although no gross dysmorphogenesis has been observed when pregnant mice are treated for the first time on GD 13, repeated administration of 2-ME that includes GD 8 (Horton *et al.*, 1985) or a single exposure on GD 8 induces exencephaly (Terry *et al.*, 1994), while 2-ME treatment of dams on GD 11 elicits digit malformations (Horton *et al.*, 1985; Clarke *et al.*, 1992). A large pharmacokinetic data base currently exists for 2-ME and 2-MAA in pregnant CD-1 mice and their conceptuses following various dosing regimens (Clarke *et al.*, 1992; Terry *et al.*, 1994). Nevertheless, the precise mechanism(s) responsible for the pharmacokinetic and pharmacodynamic behavior remains unknown.

All the models used in this study (Fig. 2) reflected the basic anatomy and physiology of the biological system. Although 2-MAA disposition in the dam was described by a nonphysiological, compartmental model, it was linked to the physiologically based model for 2-ME, where various anatomical and kinetic parameters were accurately represented. In all of the compartmental models the dam was depicted as a single compartment, and the 2-MAA concentration in maternal plasma corresponded to that in the volume of distribution. The GD 8 conceptus was also described as a single compartment because of the technical difficulties associated with the preparation of embryonic tissue for 2-MAA analyses. Dissection of individual components would have to be carried out with immersion in a buffer which could have compromised the kinetic results (Terry *et al.*, 1994). Hence, conceptus samples collected on GD 8 consisted of the combined tissues of embryo, EAF, yolk sac placenta, and decidua, whose collective weight appropriately corresponded to that derived by the physiological pregnancy model (Clarke *et al.*, 1993). For GD 11 and 13, the embryonic compartments (placenta, EAF, and embryo) were represented individually in the models, as each tissue was examined individually. Additionally, each model reflected the fundamentals of the chemical's flow such that on GD 8 passage occurred between dam and conceptus within the decidual swelling. At later gestation times, flow through the umbilical vein and arteries was represented by the communication of 2-MAA between placenta and embryo. Flow was simulated between embryo and fluid, and chemical passage between the placenta and EAF, which is believed to occur (Krauer *et al.*, 1980; Clarke *et al.*, 1993), was also represented.

The "success" or "failure" of model simulations was determined using visual judgement; there were no absolute rules

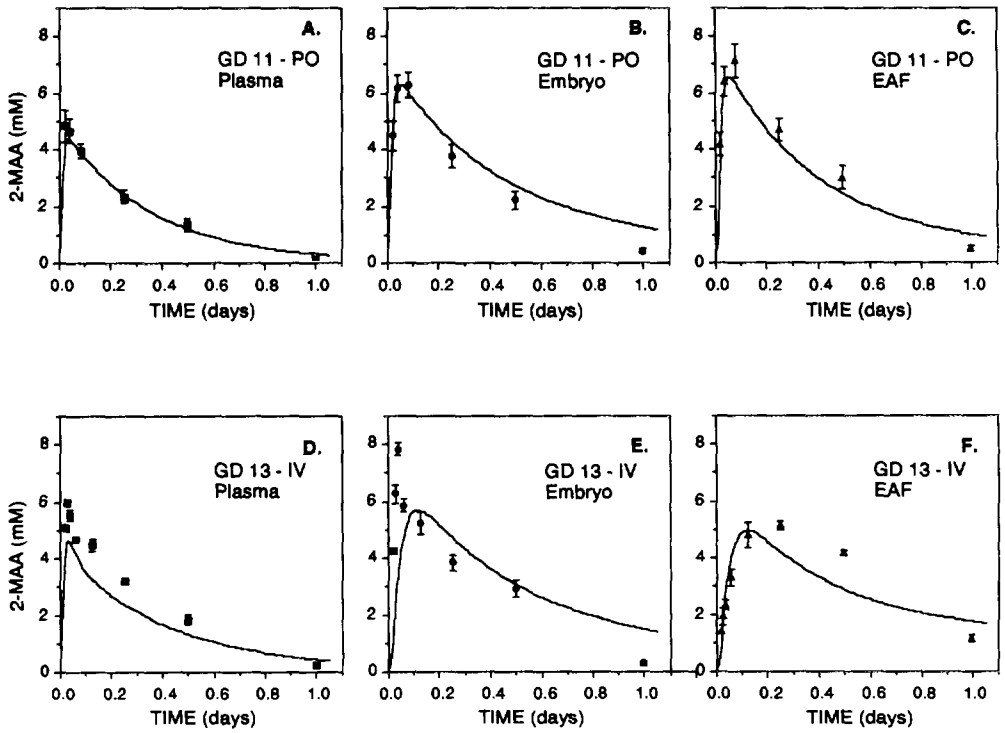

FIG. 6. Reversible binding model simulations following oral (po) administration of 250 mg 2-ME/kg on GD 11 (A–C) or intravenous (iv) injection on GD 13 (D–F). The solid lines are the simulations of 2-MAA pharmacokinetic data, and the symbols represent the biological data points (±SEM) in plasma (A and D), embryo (B and E), and extraembryonic fluid (EAF; C and F).

for assessing goodness of fit. While we acknowledge that some of the fits produced by our successful models are not perfect, the point of our modeling exercise was not to obtain flawless simulations of the data. The point was to use the process of model development as a means of learning about the system we are studying. Therefore, the issue becomes not whether the model is right or wrong, but whether it is useful.

A flow-limited model successfully simulated the pharmacokinetics of 2-MAA on GD 8 in the plasma and conceptus. Although 2-MAA transfer processes in the embryo are presently unknown, transport systems in the rodent visceral yolk sac involve fluid-phase and receptor-mediated endocytosis (Jollie, 1990). The model does not exclude the possible involvement of active transport, but suggests that the rate of 2-MAA transfer was limited by blood flow to the conceptus. This is in agreement with conclusions reached by Buelke-Sam *et al.* (1982) who reported that redistribution of blood flow had direct bearing upon yolk sac transport functions. The blood flow-limited model was not the only hypothesis evaluated at this gestation time. A more complex model depicting active transport of 2-MAA into separate embryo and EAF compartments produced better, more accurate simulations of the GD 8 conceptus kinetics. Since there were no data justifying the simulation of individual compartments, however, the model was considered an inappropriate representation of the biological sample and rejected.

Several hypotheses were unsuccessful at describing 2-MAA kinetic behavior during mid to late organogenesis. Simulations obtained with the model describing flow-limited transfer of 2-MAA on GD 11 and 13 indicated that tissue partitioning alone did not adequately account for the tissue dosimetry observed. Likewise, while highly predictive of GD 11 kinetics, the model by Clarke *et al.* (1993) failed to successfully simulate 2-MAA dosimetry on GD 13. Analysis of these models leads to the development of alternative hypotheses. Results obtained by testing one such hypothesis, the pH model, strengthened a preexisting theory. Within the developing mouse embryo, the intracellular pH (pH_i) progressively becomes more acidic, so that by GD 11, the pH_i value equals the pH of maternal plasma (Scott *et al.*, 1987). If pH partitioning alone were to determine embryonic 2-MAA disposition, the concentration of 2-MAA should be similar in maternal plasma and embryo on GD 11 (Clarke *et al.*, 1993). Kinetic data, however, do not support this as the peak 2-MAA concentration in the GD 11 embryo is 30% higher than that in the plasma (Clarke *et al.*, 1993). The fact that the pH trapping model affirmed conclusions drawn from the actual pharmacokinetics and showed clearly that pH gradients across embryonic membranes could not explain 2-MAA accumulation in the embryo increases confidence in the modeling process. Hence, our "failed" models were useful tools for learning about the system, substantiating ideas, and influencing future model development.

Since the biological basis for 2-MAA accumulation is not yet understood, "successful" models incorporated empirical modifications to simulate various transport mechanisms. Those providing the best simulations of chemical disposition on both GD 11 and 13 described active transport or reversible binding. Active transport operates against a concentration gradient and is saturable, chemically selective, and energy dependent (Klaassen and Rozman, 1991). The active transport model established a pumping action for the chemical's disposition and resulted in 2-MAA flow asymmetries consistent with the pharmacokinetic data. Although this model described movement of 2-MAA against a concentration gradient, it neither explicitly described a saturable process nor did it account for energy dependency. The reversible binding model described binding in the embryo and EAF compartments characterized by a binding maximum and a dissociation constant. The pharmacokinetics of 2-MAA on GD 11 and 13 were accurately simulated by both of these models, suggesting that active transport and/or reversible binding may play important roles in the kinetic behavior of 2-MAA at this time of mouse gestation.

While model development can help establish the likelihood of a hypothesis, it can also direct future experimental studies (Clewell and Andersen, 1985, 1989). Both the active transport and reversible binding models describe processes that lead to accumulation of 2-MAA in the appropriate target tissues. Since both models reflect the biological observations equally well, further experimental work is needed to discriminate between them. When the k_d in the reversible binding model was held constant, the binding maximum increased with developmental stage, suggesting an increase with time in the number of binding sites for 2-MAA. No significant 2-ME or 2-MAA binding to protein was detectable in whole embryo homogenate or EAF upon centrifugal filtration using radioactive 2-ME and a micropartitioning membrane in conjunction with liquid scintillation spectrometry (unpublished observations). It is conceivable, however, that a minute amount of protein contains a population of specific binding sites that would remain undetectable in the large excess of other proteins with the techniques used so far.

The first attempt by Clarke *et al.* (1993) to mathematically model 2-ME/2-MAA pharmacokinetics built upon the gestation model of O'Flaherty and co-workers (1992) and successfully described chemical dosimetry on a single day of prenatal development in mouse embryos. The present study examined alternative hypotheses, and a model was developed that could simulate pharmacokinetic behavior at various developmental stages of organogenesis. This report illustrates how simulation modeling allows the evaluation of several hypotheses when adequate data are available, and the results emphasize the need for constant reevaluations and refinements of mathematical descriptions during model development. The work demonstrates that, even when the mechanism of tissue response is not clearly understood, the quantitative relationship between chemical exposure and tissue dosimetry can be examined. By testing many hypotheses on multiple gestation days, discrimination can be made between plausible and unlikely mechanistic scenarios which may be further tested experimentally. Confidence in this model will be enhanced if interspecies extrapolations are successful. Thus, the next step in the continuing evolution of the model is to use the successful hypotheses presented here, extrapolate from mice to rats, and then validate the simulations with biological data. Further development of this PBPK model that builds on the exposure → dose → response paradigm for 2-MAA will facilitate more realistic human risk assessments for the development toxicity of 2-ME/2-MAA and related compounds.

APPENDIX I

The equations for growth of the maternal organs and conceptus are described in O'Flaherty *et al.* (1992). The work described in this report used a modified version of the O'Flaherty model (Clarke *et al.*, 1993). The PBPK model for 2-ME used in the present work was also described by Clarke *et al.* (1993). In the following, the five models for 2-MAA pharmacokinetics in the conceptus are described.

Flow-Limited, GD 8 (Fig. 2A)

The rate of change of 2-MAA in the dam (dA_{mp}/dt) is given by

$$\frac{dA_{mp}}{dt} = \frac{d\mathrm{MET}_{me}}{dt} - \frac{d\mathrm{ELIM}_{ma}}{dt} - Q\cdot\left(C_{mp} - \frac{C_{cn}}{P_{cn}}\right), \quad (1)$$

where $d\mathrm{MET}_{me}/dt$ is the rate (mmol/day) of production of 2-MAA by metabolism of 2-ME, $d\mathrm{ELIM}_{ma}/dt$ is the rate (1/day) of elimination of 2-MAA due to metabolism and urinary elimination (Clarke *et al.*, 1993), Q is the blood flow (liter/day) to the conceptus, C_{mp} is the concentration (mmol/liter) of 2-MAA in the dam, C_{cn} is the concentration (mmol/liter) of 2-MAA in the conceptus, and P_{cn} is the conceptus:blood partition coefficient. The last term of Eq. [1] describes the rate of change of 2-MAA in the conceptus. Note that, in this model, C_{mp}, the concentration of 2-MAA in the dam, is also the concentration of 2-MAA which flows in blood from the dam to the conceptus.

Flow-Limited, GD 11 and 13 (Fig. 2B)

The rate of change of 2-MAA in the placenta (dA_{pla}/dt) is given by

$$\frac{dA_{pla}}{dt} = Q\cdot\left(C_{mp} + \frac{C_e}{P_e} + \frac{C_f}{P_f} - 3\cdot\frac{C_{pla}}{P_{pla}}\right), \quad (2)$$

where C_e, C_f, and C_{pla} are the concentrations (mmol/liter) of 2-MAA in the embryo, extraembryonic fluid, and placenta, respectively. P_e, P_f, and P_{pla} are the tissue:blood partition coefficients for the embryo, extraembryonic fluid, and placenta, respectively. The rate of change of 2-MAA in the embryo (dA_e/dt) is given by

$$\frac{dA_e}{dt} = Q \cdot \left(\frac{C_{pla}}{P_{pla}} + \frac{C_f}{P_f} - 2 \cdot \frac{C_e}{P_e} \right). \quad (3)$$

The rate of change of 2-MAA in the extraembryonic fluid (dA_f/dt) is given by

$$\frac{dA_f}{dt} = Q \cdot \left(\frac{C_e}{P_e} + \frac{C_{pla}}{P_{pla}} - 2 \cdot \frac{C_f}{P_f} \right). \quad (4)$$

pH Trapping, GD 11 and 13 (Fig. 2C)

The rate of change of 2-MAA in the placental blood (dA_{plab}) is given by

$$\frac{dA_{plab}}{dt} = Q \cdot \left(C_{mp} + \frac{C_{plah}}{P_{pla}} - C_{vpla} - C_{bh} \right), \quad (5)$$

where C_{plah} is the concentration (mmol/liter) of the protonated form of 2-MAA in the placental tissue, C_{vpla} is the total concentration (mmol/liter) of 2-MAA in the placental blood, and C_{bh} is the concentration (mmol/liter) of protonated 2-MAA in the placental blood. The concentration of ionized 2-MAA in placental blood is given by the following expression which is derived from the Henderson–Hasselbalch equation:

$$C_{bh} = \frac{C_{vpla} \cdot 10^{pK_a - pH_b}}{1 + 10^{pK_a - pH_b}}, \quad (6)$$

where pK_a is the pK_a for 2-MAA and pH_b is the pH of maternal blood. The rate of change of 2-MAA in placental tissue is given by

$$\frac{dA_{pla}}{dt} = Q \cdot \left(C_{bh} + \frac{C_{eh}}{P_e} + \frac{C_{fh}}{P_f} - 3 \cdot \frac{C_{plah}}{P_{pla}} \right). \quad (7)$$

The concentration of ionized 2-MAA in placental tissue is calculated using the same form as Eq. [6]. Expressions equivalent to those for placental tissue are used for embryo and extraembryonic fluid. In all cases the flow between compartments is Q.

Active Transport, GD 11 and 13 (Fig. 2D)

The active transport model is similar to the flow-limited model for GD 11 and 13 (see above), except that Q is replaced for the embryo and extraembryonic fluid by compartment-specific flow parameters. The rate of change of 2-MAA in the placenta (dA_{pla}/dt) is given by

$$\frac{dA_{pla}}{dt} = Q \cdot \left(C_{mp} - \frac{C_{pla}}{P_{pla}} \right) + PA4 \cdot \left(\frac{C_f}{P_f} - \frac{C_{pla}}{P_{pla}} \right) + PA2 \cdot \frac{C_e}{P_e} - PA1 \cdot \frac{C_{pla}}{P_{pla}}, \quad (8)$$

where PA1, PA2, and PA4 are adjustable flow (liter/day) parameters. The rate of change of 2-MAA in the embryo (dA_e/dt) is given by

$$\frac{dA_e}{dt} = PA1 \cdot \frac{C_{pla}}{P_{pla}} + PA3 \cdot \left(\frac{C_f}{P_f} - \frac{C_e}{P_e} \right) - PA2 \cdot \frac{C_e}{P_e}. \quad (9)$$

The rate of change of 2-MAA in the extraembryonic fluid (dA_f/dt) is given by

$$\frac{dA_f}{dt} = PA3 \cdot \left(\frac{C_e}{P_e} - \frac{C_f}{P_f} \right) + PA4 \cdot \left(\frac{C_{pla}}{P_{pla}} - \frac{C_f}{P_f} \right). \quad (10)$$

Reversible Binding, GD 11 and 13 (Fig. 2E)

This model resembles the flow-limited model with the addition of reversible binding in the embryo and extraembryonic fluid compartments. The binding parameters are compartment-specific. The rate of change of 2-MAA in the placenta is given by

$$\frac{dA_{pla}}{dt} = Q \cdot \left(C_{mp} + \frac{C_{ef}}{P_e} + \frac{C_{ff}}{P_f} - 3 \cdot \frac{C_{pla}}{P_{pla}} \right), \quad (11)$$

where C_{ef} and C_{ff} are the concentrations of free (not bound) 2-MAA in the embryo and extraembryonic fluid. The rate of change of 2-MAA in the embryo is given by

$$\frac{dA_e}{dt} = Q \cdot \left(\frac{C_{pla}}{P_{pla}} + \frac{C_{ff}}{P_f} - 2 \cdot \frac{C_{ef}}{P_e} \right). \quad (12)$$

The concentration of free 2-MAA in the embryo is computed using

$$C_{ef} = \frac{A_e}{V_e + \dfrac{b_m}{k_d + C_{ef}}}, \quad (13)$$

where A_e is the total amount (mmol) of 2-MAA in the compartment, V_e is the volume of the compartment, b_m is the binding maximum (mmol/liter), and k_d is the dissociation constant (mmol/liter). Finally, the rate of change of 2-MAA in the extraembryonic fluid is given by

$$\frac{dA_f}{dt} = Q \cdot \left(\frac{C_{pla}}{P_{pla}} + \frac{C_{ef}}{P_f} - 2 \cdot \frac{C_{ff}}{P_f} \right) \quad (14)$$

and the concentration of free 2-MAA in the extraembryonic fluid is calculated using an expression equivalent to Eq. [13].

APPENDIX II

Parameter Values for Simulations Shown in Fig. 4 (Flow-Limited, GD 8)

Parameter	Value	Reference
Blood flow to placenta (liter/day)	0.26	Blood flow to total litter conceptuses; see Results for explanation
Conceptus/blood PC	1.07	See Table 3
K_e (day $^{-1}$)	1.97	See Table 1
K_f (day $^{-1}$)	1.12	See Table 1

Parameter Values for Simulations Shown in Fig. 5 (Active Transport)

Parameter	Value	Reference
GD 11		
Blood flow to placenta (liter/day)	0.15	Blood flow to total litter conceptuses; see Results for explanation
Placenta/blood PC	1.05	See Table 3
Embryo/blood PC	0.94	See Table 3
EAF/blood PC	1.33	See Table 3
K_e (day $^{-1}$)	1.92	See Table 1
K_f (day $^{-1}$)	1.10	See Table 1
PA1 (liter/day)	1.15	Visually optimized; see Appendix I for use
PA2 (liter/day)	0.63	Visually optimized; see Appendix I for use
PA3 (liter/day)	0.70	Visually optimized; see Appendix I for use
PA4 (liter/day)	0.30	Visually optimized; see Appendix I for use
GD 13		
Blood flow to placenta (liter/day)	0.29	Blood flow to total litter conceptuses; see Results for explanation
Placenta/blood PC	1.33	See Table 3
Embryo/blood PC	1.26	See Table 3
EAF/blood PC	1.11	See Table 3
K_e (day $^{-1}$)	1.87	See Table 1
K_f (day $^{-1}$)	1.06	See Table 1
PA1 (liter/day)	1.15	Visually optimized; see Appendix I for use
PA2 (liter/day)	0.63	Visually optimized; see Appendix I for use
PA3 (liter/day)	0.70	Visually optimized; see Appendix I for use
PA4 (liter/day)	0.30	Visually optimized; see Appendix I for use

Parameter Values for Simulations Shown in Fig. 6 (Reversible Binding)

Parameter	Value	Reference
GD 11		
Blood flow to placenta (liter/day)	0.15	Blood flow to total litter conceptuses; see Results for explanation
Placenta/blood PC	1.05	See Table 3
Embryo/blood PC	0.94	See Table 3
EAF/blood PC	1.33	See Table 3
K_e (day $^{-1}$)	1.92	See Table 1
K_f (day $^{-1}$)	1.10	See Table 1
K_d (mmol/liter)	0.0008	Visually optimized; see Appendix I for use
B_m (mmol)	0.0008	Visually optimized; see Appendix I for use
GD 13		
Blood flow to placenta (liter/day)	0.29	Blood flow to total litter conceptuses; see Results for explanation
Placenta/blood PC	1.33	See Table 3
Embryo/blood PC	1.26	See Table 3
EAF/blood PC	1.11	See Table 3
K_e (day $^{-1}$)	1.87	See Table 1
K_f (day $^{-1}$)	1.06	See Table 1
K_d (mmol/liter)	0.0008	Visually optimized; see Appendix I for use
B_m (mmol)	0.003	Visually optimized; see Appendix I for use

ACKNOWLEDGMENTS

The authors express their appreciation to Dr. David Dorman, Mr. Donald Stedman, and Mr. Michael Terry for their insight and helpful comments regarding the manuscript. This work was supported in part by NIEHS-NIH Grant 1 F32 ES05601-01 PSF awarded to K. K. (White) Terry.

REFERENCES

Andersen, M. E., Clewell, H. J., Gargas, M. L., Smith, F. A., and Reitz, R. H. (1987). Physiologically based pharmacokinetics and the risk assessment process for methylene chloride. *Toxicol. Appl. Pharmacol.* **87**, 185–205.

Brown, N. A., Holt, D., and Webb, M. (1984). The teratogenicity of methoxyacetic acid in the rat. *Toxicol. Lett.* **2**, 93–100.

Buelke-Sam, J., Holson, J. F., and Nelson, C. J. (1982). Blood flow during pregnancy in the rat: II. Dynamics of and litter variability in uterine flow. *Teratology* **26**, 279–288.

Clarke, D. O., Duignan, J. M., and Welsch, F. (1992). 2-Methoxyacetic acid dosimetry–teratogenicity relationships in CD-1 mice exposed to 2-methoxyethanol. *Toxicol. Appl. Pharmacol.* **114**, 77–87.

Clarke, D. O., Elswick, B. A., Welsch, F., and Conolly, R. B. (1993). Pharmacokinetics of 2-methoxyethanol and 2-methoxyacetic acid in the pregnant mouse: A physiologically based mathematical model. *Toxicol. Appl. Pharmacol.* **121**, 239–252.

Clewell, H. J., and Anderson, M. E. (1985). Risk assessment extrapolations and physiological modeling. *Toxicol. Ind. Health.* **1**, 111–131.

Clewell, H. J., and Andersen, M. E. (1989). Improving toxicology testing protocols using computer simulations. *Toxicol. Lett.* **49**, 139–158.

Conolly, R. B., and Andersen, M. E. (1991). Biologically based pharmacodynamic models: Tools for toxicological research and risk assessment. *Annu. Rev. Pharmacol. Toxicol.* **31,** 503–523.

Fisher, J. W., Whittaker, T. A., Taylor, D. H., Clewell, H. J., and Andersen, M. E. (1989). Physiologically based pharmacokinetic modeling of the pregnant rat: A multiroute exposure model for trichloroethylene and its metabolite, trichloroacetic acid. *Toxicol. Appl. Pharmacol.* **99,** 395–414.

Gabrielsson, J. L., and Paalzow, L. K. (1983). A physiological pharmacokinetic model for morphine disposition in the pregnant rat. *J. Pharmacokinet. Biopharm.* **11,** 147–163.

Gabrielsson, J., and Larsson, K. S. (1987). The use of physiological pharmacokinetic models in studies on the disposition of salicylic acid in pregnancy. In *Pharmacokinetics in Teratogenesis* (H. Nau and W. J. Scott, Eds.), pp. 13–25. CRC Press, Boca Raton, FL.

Gabrielsson, J. L., Paalzow, L. K., and Nordstrom, L. (1984). A physiologically based pharmacokinetic model for theophylline disposition in the pregnant and nonpregnant rat. *J. Pharmacokinet. Biopharm.* **12,** 149–164.

Gabrielsson, J. L., Johansson, P., Bondesson, U., and Paalzow, L. K. (1985). Analysis of methadone disposition in the pregnant rat by means of a physiological flow model. *J. Pharmacokinet. Biopharm.* **13,** 355–372.

Gabrielsson, J. L., Johansson, P., Bondesson, U., Karlsson, M., and Paalzow, L. K. (1986). Analysis of pethidine disposition in the pregnant rat by means of a physiological flow model. *J. Pharmacokinet. Biopharm.* **14,** 381–395.

Himmelstein, K. J., and Lutz, R. J. (1979). A review of the application of physiologically based pharmacokinetic modelling. *J. Pharmacokin. Biopharm.* **7,** 127–145.

Horton, V. L., Sleet, R. B., John-Greene, J. A., and Welsch, F. (1985). Developmental phase-specific and dose-related teratogenic effects of ethylene glycol monomethyl ether in CD-1 mice. *Toxicol. Appl. Pharmacol.* **80,** 108–118.

Jepson, G. W., Hoover, D. K., Black, R. K., McCafferty, J. D., Mahle, D. A., and Gearhart, J. M. (1994). A partition coefficient determination method for nonvolatile chemicals in biological tissues. *Fundam. Appl. Toxicol.* **22,** 519–524.

Jollie, W. P. (1990). Development, morphology, and function of the yolk-sac placenta of laboratory rodents. *Teratology* **41,** 361–381.

Klaassen, C. D., and Rozman, K. (1991). Absorption, distribution, and excretion of toxicants. In *Casarett and Doull's Toxicology: The Basic Science of Poisons* (M. O. Amdur, J. Doull, and C. D. Klaassen, Eds.), pp. 50–87. Pergamon, Elmsford, NY.

Krauer, B., Krauer, F., and Hytten, F. E. (1980). Drug disposition and pharmacokinetics in the maternal-placental-fetal unit. *Pharmacol. Ther.* **10,** 301–328.

Nau, H. (1985). Teratogenic valproic acid concentrations: Infusion by implanted minipumps vs conventional injection regiment in the mouse. *Toxicol. Appl. Pharmacol.* **80,** 243–250.

O'Flaherty, E. J., Scott, W., Schreiner, C., and Beliles, R. P. (1992). A physiologically based kinetic model of rat and mouse gestation: Disposition of a weak acid. *Toxicol. Appl. Pharmacol.* **112,** 245–256.

Olanoff, L. S., and Anderson, J. M. (1980). Controlled release of tetracycline-III: A physiological pharmacokinetic model of the pregnant rat. *J. Pharmacokinet. Biopharm.* **8,** 599–620.

Ritter, E. J., Scott, W. J., Randall, J. L., and Ritter, J. M. (1985). Teratogenicity of dimethoxyethyl phthalate and its metabolites methoxyethanol and methoxyacetic acid in the rat. *Teratology* **32,** 25–31.

Scott, W. J., Duggan, C. A., Schreiner, C. M., Collins, M. D., and Nau, H. (1987). Intracellular pH of rodent embryos and its association with teraogenic response. In *Approaches to Elucidate Mechanisms in Teratogenesis* (F. Welsch, Ed.), pp. 99–107. Hemisphere, Washington, DC.

Scott, W. J., Duggan, C. A., Schreiner, C. M., and Collins, M. D. (1990). Reduction of embryonic intracellular pH: A potential mechanism of acetazolamide-induced limb malformations. *Toxicol. Appl. Pharmacol.* **103,** 238–254.

Sleet, R. B., Greene, J. A., and Welsch, F. (1988). The relationship of embryotoxicity to disposition of 2-methoxyethanol in mice. *Toxicol. Appl. Pharmacol.* **93,** 195–207.

Terry, K. K., Elswick, B. A., Stedman, D. B., and Welsch, F. (1994). Developmental phase alters dosimetry–teratogenicity relationship for 2-methoxyethanol in CD-1 mice. *Teratology* **49,** 218–227.

Wegner, C., and Nau, H. (1992). Alteration of embryonic folate metabolism by valproic acid during organogenesis: Implications for mechanism of teratogenesis. *Neurology* **42,** 17–24.

Yonemoto, J., Brown, N. A., and Webb, M. (1984). Effects of dimethoxyethyl phthalate, monomethoxyethyl phthalate, 2-methoxyethanol and methoxyacetic acid on post implantation rat embryos in culture. *Toxicol. Lett.* **21,** 97–102.